ELSEVIER

Journal of Alloys and Compounds 444–445 (2007) 533–539

Journal of ALLOYS AND COMPOUNDS

www.elsevier.com/locate/jallcom

Plutonium uptake by brucite and hydroxylated periclase

John Douglas Farr [a,*], Mary P. Neu [a], Roland K. Schulze [a], Bruce D. Honeyman [b]

[a] *Los Alamos National Laboratory, Nuclear Materials Science, MST-16, MS G721, Los Alamos, NM 87544, USA*
[b] *Colorado School of Mines, Golden, CO 80401, USA*

Received 12 September 2006; received in revised form 15 November 2006; accepted 16 November 2006
Available online 29 December 2006

Abstract

Batch adsorption experiments and spectroscopic investigations consistently show that aqueous Pu(IV) is quickly removed from solution and becomes incorporated in a brucite or hydroxylated MgO surface to a depth of at least 50 nm, primarily as Pu(IV) within a pH range of 8.5–12.5, and is unaffected by the presence of the organic ligand, citrate. X-ray photoelectron spectroscopy (XPS), X-ray absorption fine structure (XAFS) and Rutherford backscattering spectroscopy (RBS) were used to estimate Pu penetration depth and provide information about its chemical state.

Keywords: Actinide compounds; Surfaces and interfaces; Liquid–solid reactions; XPS; RBS

1. Introduction

Actinides may become associated with the surfaces of minerals through a variety of processes, including surface complexation [1,2], incorporation or mineralization [3–6], by surface precipitation, or a combination of these processes [7,8]. Previous work [9] showed that Pu(IV) was quickly and completely removed from solution by colloidal brucite ($Mg(OH)_2$). Surface analysis (by X-ray photoelectron spectroscopy (XPS)) of natural crystalline brucite and hydroxylated MgO (1 0 0) substrates exposed to aqueous Pu(IV) showed that Pu was incorporated in these minerals to significant depths. The investigations described below were designed to further determine the physical and chemical nature of absorbed Pu using both surface-sensitive and bulk analysis techniques.

These experiments were conducted so that the results could be correlated to batch sorption experiments as closely as possible. A variety of Pu(IV) exposure conditions were chosen to help understand the effects of differences in experimental conditions dictated by these ex situ spectroscopic experiments. The most substantial difference between the solution phase experiments from the previous work and the experiments discussed below is that much higher Pu(IV) solution concentrations were needed here to accommodate the detection limits in the various spectroscopic techniques used.

2. Methods and materials

Materials used in this part of the study were colloidal brucite, natural crystalline brucite and hydroxylated MgO (1 0 0) single crystals. The MgO (1 0 0) single crystals were hydroxylated to a depth of about 50 Å by evaporating low-carbon deionized water on the surface under an inert atmosphere. X-ray photoelectron spectroscopy was the primary method used to determine the nature of the adsorbed Pu. Several other techniques (described below) were used to provide additional and corroborating information, particularly about the penetration depth of Pu.

A Kratos XSAM 800 X-ray photoelectron spectrometer system was used to collect the XPS data. High-resolution spectra were acquired at 20 eV pass energy using Mg Kα X-rays and an acceptance half-angle of 25°. No electron flood gun charge compensation was used in these measurements. Charge correction was performed by referencing the adventitious (hydrocarbon-like) carbon to 284.6 eV binding energy. Atomic concentration estimates were based on sensitivity factors appropriate for the instrumental conditions and analyzer design. The binding energy values and sensitivity factor used for the Pu 4f region were based on data derived from known Pu compounds, including PuO_2 [10], $Pu(OH)_4$ [11] and PuF_4 [12]. X-ray absorption near-edge structure (XANES) was used for determining the oxidation state of Pu in the materials. X-ray absorption fine structure (XAFS) yielded some information about local bonding and inter-atomic distances. Pu L_3 X-ray data was collected at the Stanford Synchrotron Research Laboratory. Rutherford backscattering spectroscopy (RBS) was used to determine the penetration depth of Pu in MgO (1 0 0) crystals. This is an ideal technique for the analysis of heavy elements in a light matrix. These experiments were done using alpha particles (He nuclei) accelerated at 5.5 MeV in the Ion Beam Materials Laboratory at LANL.

3. Results and discussion

Two sets of MgO (1 0 0) single crystals and natural crystalline brucite samples were immersed in 1×10^{-5} M ^{239}Pu(IV)

* Corresponding author. Tel.: +1 505 667 4033; fax: +1 505 667 1058.
E-mail address: d.farr@lanl.gov (J.D. Farr).

0925-8388/$ – see front matter © 2006 Elsevier B.V. All rights reserved.
doi:10.1016/j.jallcom.2006.11.176

Table 1
Sample descriptions showing the experimental parameters and estimated quantities of Pu sorbed

Sample	Substrate	Initial/final pH	Exposure time (h)	Estimated mass/activity ^{239}Pu
9	$Mg(OH)_2$	0/Not measured	7	6×10^{-9} g/4×10^{-10} Ci
8	$Mg(OH)_2$	2/Not measured	7	6×10^{-9} g/4×10^{-10} Ci
13	MgO	0/Not measured	7	2×10^{-8} g/1×10^{-9} Ci
14	MgO, SiO_2	2/Not measured, 0/not measured	7, 7	1×10^{-9} g/6×10^{-10} Ci, 6×10^{-9} g/4×10^{-10} Ci
1	$Mg(OH)_2$	2.2/8.13	70	3×10^{-7} g/2×10^{-8} Ci
3	$Mg(OH)_2$	8.5/8.4	70	1×10^{-7} g/6×10^{-9} Ci
4	MgO	2.2/8.8	70	1×10^{-7} g/6×10^{-9} Ci
2	MgO	9.1/9.2	70	3×10^{-7} g/2×10^{-8} Ci

in 1 M $HClO_4$ for two different time periods (7 and 70 h), then rinsed with Mg(II)-saturated DI water to remove loosely bound species and allowed to air-dry. For comparison, an oxidized silicon wafer was also exposed to the same solution conditions for 7 h. The results of this experiment sharply contrast with those from MgO or brucite exposed to Pu(IV) to illustrate differences in substrate/adsorbate behavior. Oxidized Si wafers do not dissolve like the MgO or brucite substrates, so any Pu adsorbed will remain on the surface. Table 1 lists the sample descriptions, their respective exposure conditions and the estimated quantity of Pu sorbed, based on alpha counting.

All of the MgO (1 0 0) substrates were hydroxylated before the Pu exposure to an estimated depth of 40 Å, as measured by XPS, by evaporating a drop of low carbon deionized water on their surfaces. The brucite crystals were immersed in the Pu(IV) solutions immediately after being cleaved in air. Upon drying, estimates of the quantity of sorbed Pu were obtained by alpha counting using a probe set at a fixed distance above the samples. The results of this measurement technique and its implications are discussed below.

Exposure of these crystals to a strong acid will quickly result in dissolution, so attempts were made to minimize this process by raising the initial pH of some of the solutions. This is a necessary compromise that is driven on one hand by the need to maintain high Pu concentrations that will be primarily in the (IV) state and the desire on the other hand to approach the near-neutral pH values seen in the real world. The initial pH of the Pu-containing solutions was measured for all of the samples. For both sets of samples, solutions that had two different pH values were used. For the 7 h batch, initial pH's were around 0 for a brucite and a MgO crystal and about 2 for the other brucite and MgO samples. Although pH 2 is still rather acidic compared to the expected pH in real systems, it represents a step in that direction.

The samples exposed to pH 2 initially gave much better XPS results (greater intensity for the Pu 4f region, meaning more surface Pu) than the samples that started at pH's around 0. This was interpreted as an indication of less surface dissolution and damage to the crystals exposed initially to pH 2. Both brucite samples had comparable amounts of sorbed Pu, based on alpha counting, but no useful data could be obtained for Pu from the low pH sample because the signal was so weak. The low pH MgO sample had about an order of magnitude more activity, but the XPS data for Pu for this sample was only marginal, at only a few tenths of an atomic percent, indicating that the Pu had been incorporated in the crystal below the surface. Pu sorbs well at these extremely low pH's according to the alpha counting results, in fact, it sorbs too effectively to be observed by a surface-sensitive technique.

Much higher initial pH values were used for selected samples in the 70-h batch. One of the cleaved brucite crystals was immersed in a solution with an initial pH of 8.5, and a hydroxylated MgO sample was placed in a solution that had an initial pH of 9.1. The other brucite and MgO crystals in the 70-h batch were in solutions that had an initial pH's of 2.2. Final pH measurements were made on these samples. They were all in the relatively basic range of 8 or 9, indicating dissolution of the substrates that were exposed to an initial pH of 2.2. Samples that started at higher pH values showed virtually no change in pH after 70 h. Final pH measurements were not obtained for the 7-h batch, but were undoubtedly much higher than at the beginning of the exposure period. For solutions with an initial pH of about 0, the primary aquo ion is expected to be Pu^{4+}. At pH 2, hydrolysis will create a mixture of $PuOH^{3+}$, $Pu(OH)_2{}^{2+}$, $Pu(OH)^{3+}$ as well as the neutral aqueous species $Pu(OH)_4$ which becomes dominant at the higher pH values used [13].

Sample preparation for these experiments deviated from the conditions used in the batch experiments in several respects. Higher Pu solution concentrations were needed to assure detection by XPS. In order to get reliable information about the chemistry of surface species, concentrations of the elements of interest at or near the surface must be at least 0.1 at.%, thus acidic solutions were used to maintain these higher Pu concentrations. There are strong correlations, however, between the spectroscopic sample conditions and the conditions that were used for in the low pH (8–9) region of the batch experiments of the previous work [9]. In those experiments, a small amount of Pu(IV) in acid was quickly injected and mixed with the alkaline, brucite-containing solutions in the centrifuge tubes. The local environment near the surfaces of the brucite crystals (whether they are in bulk or colloidal form) will be alkaline, probably near pH 10. Pu ions exposed to this elevated pH will tend to hydrolyze immediately and then adsorb on the brucite surface. The polymerization reaction for Pu at 10^{-8} M is slow, so colloid formation under the batch sorption conditions is expected to be negligible [14].

Solutions containing Pu(IV) and crystalline brucite or hydroxylated MgO crystals for the spectroscopic studies started at low pH, but became more alkaline over the course of exposure, finally reaching measured pH values between 8 and 9. As

in the batch experiments, Pu ions were presumed to have been exposed to a highly alkaline micro-environment near the surfaces of the crystals. The higher Pu concentrations used for the spectroscopic experiments, 10^{-5} M Pu(IV), may result in some Pu(IV) colloid formation. Colloidal Pu(IV) could then adsorb on the outermost layers of the substrates.

The crystals are well rinsed with Mg-saturated solutions (pH 10.2) when removed from the Pu solutions. This process is required to wash away electrolyte (acid) deposits that would interfere with the XPS analysis. Weakly bound Pu is also removed, leaving only the relevant inner sphere adsorbed Pu complexes, or Pu that was incorporated into the crystal. These strongly bound species are extremely important with respect to transport. Whether they are bound to mineral colloids or immobilized on a stable substrate, reliable predictions about their environmental mobility depends on this strong association.

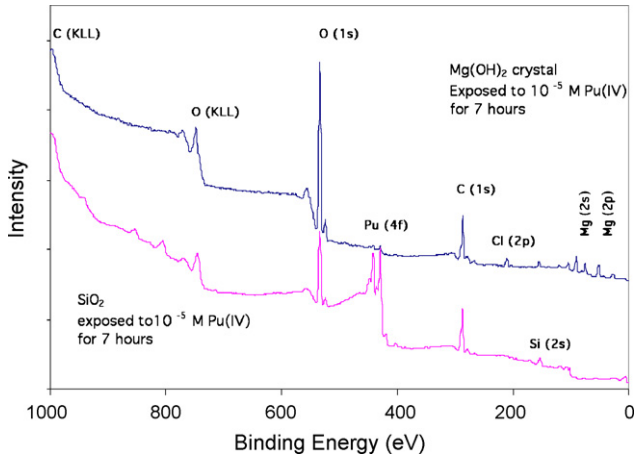

Fig. 1. XPS Surveys of brucite and SiO_2 exposed to 1×10^{-5} M Pu(IV) for 7 h. The surface concentration of Pu on the brucite crystal is less than 1 at.% and about 10 at.% on the SiO_2. Comparable alpha counts from both samples indicate the presence of subsurface Pu for brucite.

3.1. Pu sorption estimates by alpha counting

After drying in air, alpha activity was monitored by a probe that was set a fixed distance above the samples. These simple surveys showed alpha activity ranging from a few hundred to a few thousand counts per minute, yielding rough measures of Pu sorption levels. The range for 5 MeV alpha particles in brucite is about 5×10^4 nm, according to TRIM simulations [15], so alpha surveys can detect Pu below the surface at significant depths. XPS, on the other hand, is sensitive only to the outermost atomic layers. For these investigations, the analysis depth was about 4 nm.

Pu surface concentrations on sample #9, measured by XPS (which has a much shallower analysis depth than the alpha activity measurements by a factor of 10^4), were estimated at less than 1 at.%. These results sharply contrast with measurements made on the oxidized silicon wafer that had been exposed to the same Pu(IV) solution and showed nearly the same alpha activity after exposure as the brucite. Photoemission intensity for the Pu 4f lines from the SiO_2 surface were an order of magnitude higher than those from brucite, yielding concentration estimates of 10 at.% on the surface. These results, shown in Fig. 1, suggest that Pu was incorporated in the brucite subsurface, with most of the Pu being deeper than the analysis depth of XPS, but still detectable in the alpha emission.

The samples that were exposed for 7 h showed a lower overall alpha activity than the ones that were immersed for 70 h, indicating less uptake of Pu, but had higher surface Pu concentrations than the ones that were exposed for 70 h, as determined by XPS. This suggests that as exposure time increased, the sorbed Pu went deeper into the subsurface. In the cases where the pH remained essentially constant, some dissolution of the solids is also expected, although probably to a much reduced degree compared to the samples that were in very acidic solutions.

3.2. XPS results: MgO (1 0 0)

Information about the chemical state of Pu in the outermost layers of the samples listed in Table 1 was obtained by analysis of the Pu 4f core level. Fig. 2 shows spectra from several different photoemission angles from the surface of a hydroxylated MgO (1 0 0) crystal exposed to 1×10^{-5} M Pu(IV) for 7 h (sample #14). The spin-orbit splitting of the 4f level is apparent in the 5/2 and 7/2 peaks seen at about 439 and 426 eV, respectively. Pu(IV) is the dominant oxidation state, as evidenced by the distinctive satellites seen about 7 eV above the main two peaks, with a chemical shift between that expected for Pu hydroxide and Pu dioxide.

Angle dependent photoemission measurements also supported the concept of Pu subsurface incorporation. XPS showed that Pu was distributed throughout the analysis depth of about 40 Å, and was only slightly more concentrated in the outermost layers. The analysis depth was varied from about 20 Å to about 40 Å as the photoelectron take-off angle was adjusted from 30 to 90° in 20° increments. Pu/Mg atomic ratio estimates, derived from peak areas for the Pu $4f_{7/2}$ and Mg 2p regions, ranged from 0.03 for the 30° take-off angle to 0.02 for the 90° angle. As the effective analysis depth becomes shallower at 30°, Pu shifts slightly from the more ionic hydroxide-like form towards a more covalent dioxide-like state.

This indication of less hydroxylation of Pu on the surface than in the bulk goes against what one might expect for a sample that has been in such a hydroxide-rich environment, particularly if Pu(IV) colloids have adsorbed or formed on the surface. Binding energies measured on two different Pu(IV) colloid preparations [11] were higher than those expected for the dioxide, closer to those observed for $Pu(OH)_4$ or PuO_{2+x}. The apparent reduction of the surface may be an artifact of the analysis technique. Surfaces exposed to high vacuum and X-ray fluxes are liable to be reduced. The rather broad distribution of the Pu $4f_{7/2}$ region encompasses at least two different chemical states, based on curve fitting results. Two of these states are consistent with Pu(IV) as dioxide (425.5 eV) and as hydroxide (426.8 eV), together comprising over 90% of the total area under the Pu $4f_{7/2}$ peak plus the area under the satellite peak associated with it, seen at about 433 eV. There is some intensity that trails off

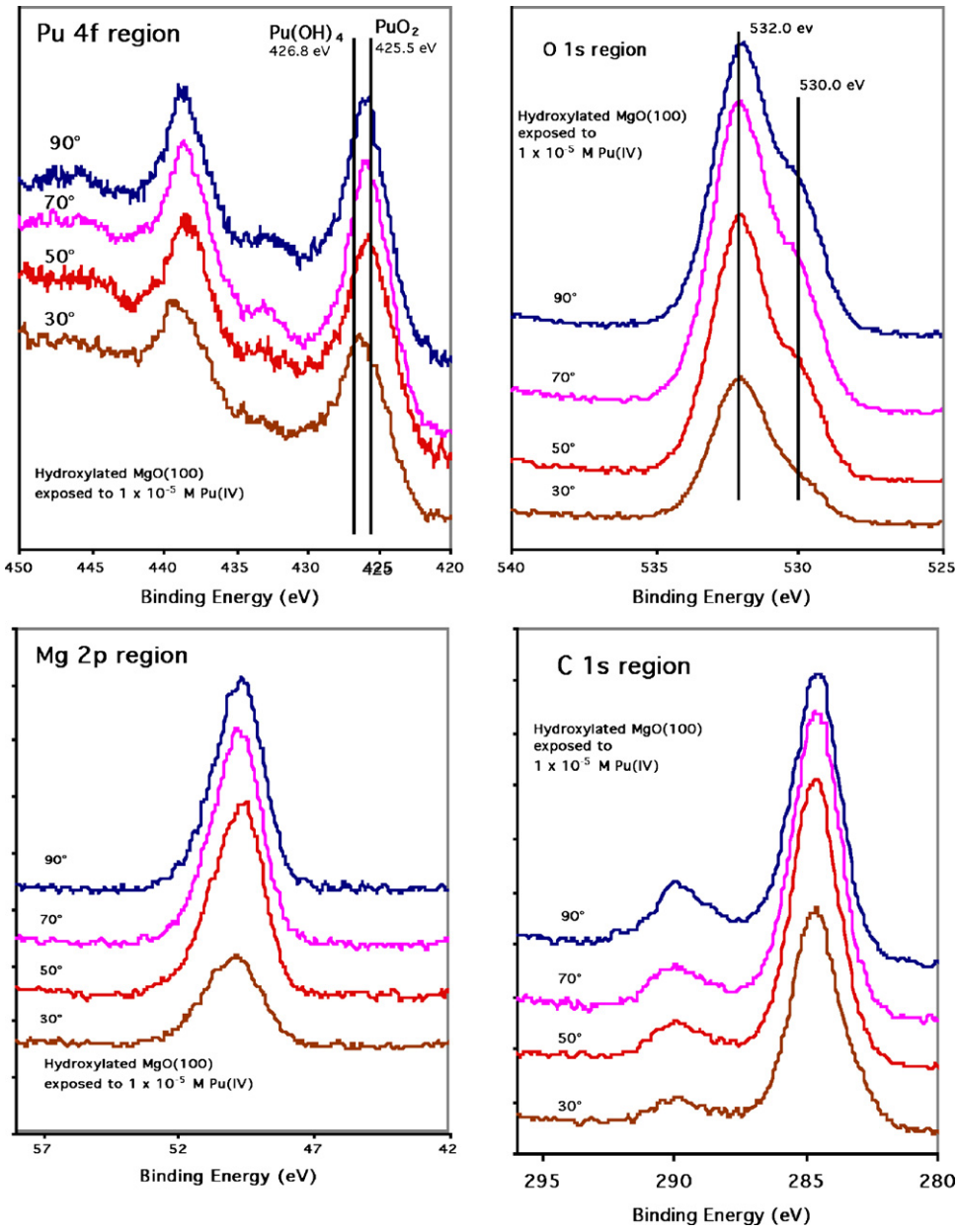

Fig. 2. Angle dependent XPS data. This data was collected from the Pu 4f, O 1s and C 1s regions for sample #14, hydroxylated MgO (1 0 0) exposed to 1×10^{-5} M Pu(IV) for 7 h.

at low binding energies, suggesting a small amount of Pu(III). This feature is slightly more prominent in data from 30° than from 90°, indicating that it is more abundant on the surface. Vacuum and X-ray induced decomposition of hydroxyls may be the explanation for the presence of Pu(III). XPS estimates of Pu concentrations were less than 1 at.%, although alpha counts were high, indicating that Pu was incorporated in the bulk.

O 1s spectra from the same analysis showed both oxide and hydroxide chemical states on the surface. As expected, the intensity for the oxide at a binding energy of about 530 eV decreases with respect to the distribution at about 532 eV along with the photoelectron take-off angle as the effective sampling depth becomes shallower. This rather broad distribution includes the value expected for brucite (531.6 eV) as well as that expected for $MgCO_3$. C 1s spectra show two peaks—adventitious carbon at 284.6 eV and a less intense peak at 290.0 eV providing evidence of surface carbonate formation. An estimate of the carbonate to hydroxide ratio, based on curve fitting that was performed on data from the O 1s and C 1s regions from the 90° photoelectron take-off angle was about 1:1.

3.3. XPS results: 70 h set

Crystals exposed for the longer time period (70 h) showed higher alpha activity by nearly an order of magnitude than those exposed for only 7 h, indicating a continuation of the high rate of Pu sorption and incorporation. Unfortunately, this apparent increase in Pu sorption was not seen in the XPS results, shown

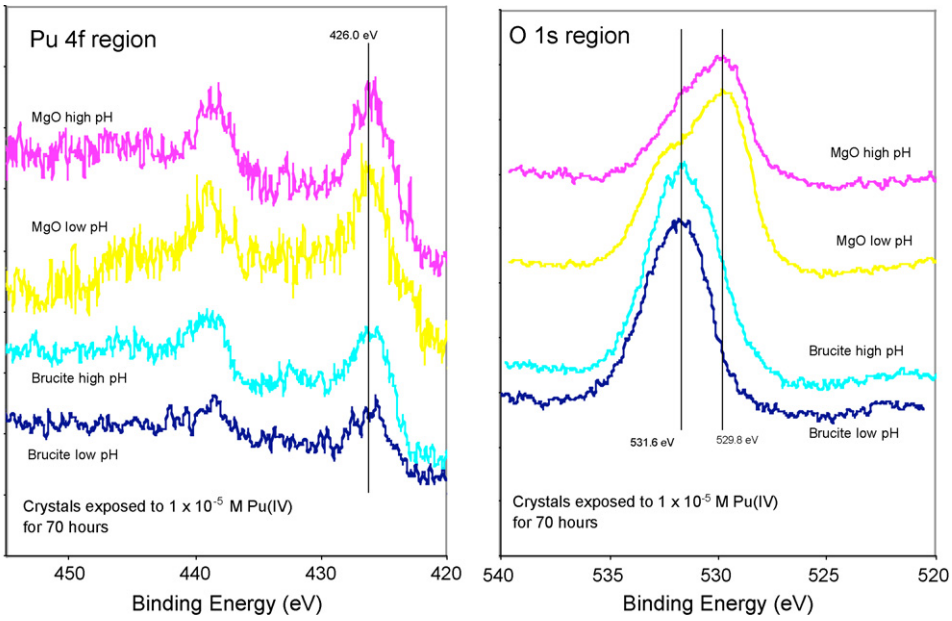

Fig. 3. XPS spectra for Pu 4f and O 1s regions of the MgO and brucite crystals that were exposed to 1×10^{-5} M Pu(IV) for 70 h. Pu intensities are less than those seen for crystals exposed for only 7 h, but alpha activity is much greater, indicating more subsurface Pu oxides and hydroxides.

in Fig. 3. In fact, Pu was barely detectable on the surfaces of all of the samples. Concentrations of surface Pu was about 0.1 at.%, again indicating that most of the Pu had become incorporated in the bulk of the crystals and was below the 40 Å analysis depth of XPS.

Low Pu concentrations and the resultant lower signal to noise ratio made chemical state identification more difficult and somewhat less certain, but the results generally were the same as in the 7-h exposure. Pu 4f intensities for these samples, shown in Fig. 3, are rather broad, but the overall binding energy of 426 eV for the $4f_{7/2}$ peak and weak but still discernable satellite features about 7 eV above the main peaks are again consistent with a mixture of Pu(IV) oxides and hydroxides. As with the 7-h batch, there was some intensity at lower binding energies again, suggesting reduced Pu perhaps as Pu(III). This effect was somewhat more pronounced than before, suggesting that the required longer X-ray exposure time during the analysis had some influence. The O 1s region shows the familiar hydroxide intensity at about 532 eV for the brucite crystals and the broader distribution for both oxide (about 530 eV) and hydroxide species that are typical for MgO crystals exposed to water.

Differences seen with these samples compared to the 7 h set were lower surface C concentrations and the appearance of more lattice oxide (with respect to hydroxide) on the MgO (1 0 0) substrates. These effects were enhanced somewhat for the low pH sample, perhaps due to the longer duration of the dissolution reactions. The O 1s peak shape is more reminiscent of those seen for crystals that were simply immersed in low-C water for 2 days. This implies that either the surface hydroxide layer is relatively thin or there may be significant roughening of the surface, producing islands of hydroxides and areas of exposed MgO. No significant differences were observed for the brucite substrates, except for the lower surface Pu concentrations.

3.4. Brucite XANES and EXAFS

X-ray absorption near-edge spectroscopy has been shown to be useful for determining Pu valence. The energies of the absorption edge and peak and the shape of the peak shown in Fig. 4 are strongly correlated with the valence and local environment of the absorbing atom [16]. Spectra obtained from a brucite crystal that was exposed to 10^{-5} M Pu(IV) for 7 h is compared to the results from an air-exposed Pu metal sample. There are no apparent differences between the two spectra, indicating Pu is in the +4 oxidation state. Extended X-ray absorption fine structure (EXAFS) analyses performed on this data set resulted in an estimated Pu–O distance of 2.3 Å, the same as that expected for PuO_2 [17]. Unfortunately, the data quality and intensity were not conducive to further interpretation.

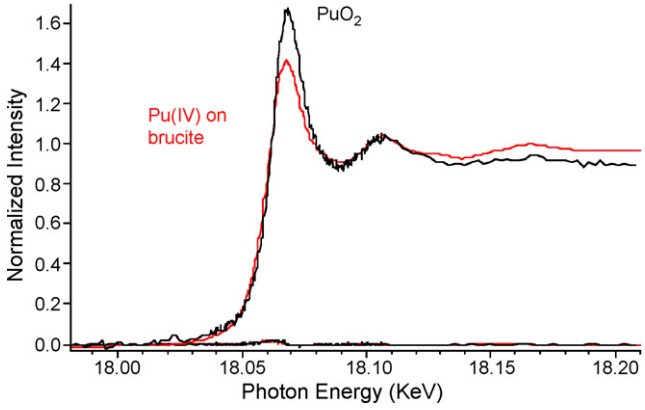

Fig. 4. Pu L_3 X-ray absorption near-edge (XANES) spectrum. The overlapping spectra illustrate the similarities between Pu(IV) adsorbed on brucite and oxidized Pu metal. Peak energy is 18,068 eV.

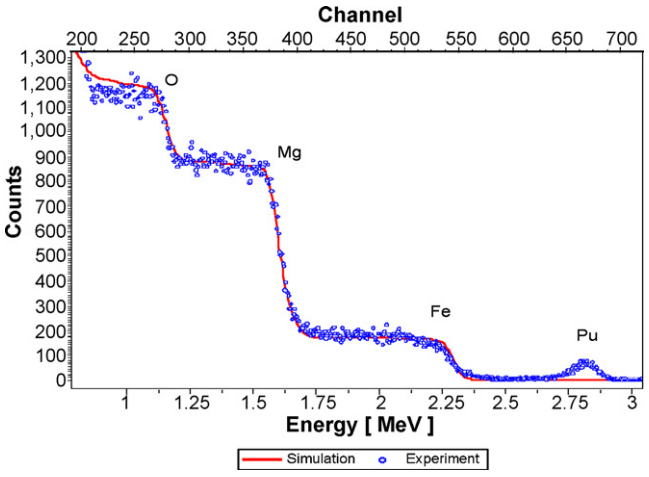

Fig. 5. Rutherford backscattering spectroscopy. Pu was detected 60–100 nm below the surface of the hydroxylated MgO (1 0 0) crystal. The sample holder is the source of the Fe signal.

3.5. Rutherford backscattering spectroscopy

This technique is well suited for analysis of heavy elements in a light matrix. Alpha particles accelerated at 5.5 MeV pass through a thin Ti foil and penetrate the MgO crystal, scattering as they encounter atoms in the solid. The energy of the backscattered particles is proportional to the mass of the atom encountered in the crystal. A plot of the number of backscattered particles as a function of their energy is shown in Fig. 5.

The energy and shape of the Pu peak is shifted to slightly lower values than would be expected if it was all on the surface. The shift to lower energy indicates that it is 60–100 nm below the hydroxylated MgO surface, thus more confirmatory evidence for Pu uptake.

4. Conclusions

Batch adsorption experiments and spectroscopic investigations consistently show that aqueous Pu(IV) is quickly removed from solution and becomes incorporated in a brucite or hydroxylated MgO surface to a depth of at least 50 nm, primarily as Pu(IV) within a pH range of 8.5–12.5. This absorption behavior is unaffected by the presence of the organic ligand, citrate [9].

Further studies on colloidal brucite, brucite crystals and MgO crystals that were exposed for longer times (70 h) to solutions containing Pu(IV) confirmed the presence of subsurface Pu and demonstrated a continuation of the Pu uptake behavior previously observed. X-ray photoelectron spectroscopy, X-ray absorption fine structure, Rutherford backscattering spectroscopy were used to estimate Pu penetration depth and provide information about its chemical state.

The initial adsorption of Pu(IV) is expected to occur rapidly due the easy availability of sorption sites on the hydroxylated MgO and brucite surfaces. In most systems, sorption of cations will commence at the pH of initial hydrolysis. The first hydrolysis constant for Pu +4 is 0.6 [18], so hydrolysis and adsorption occur below pH 1. Under the solution conditions of these experiments, Pu will exist primarily as the neutral tetra hydroxide [18]. The MgO and brucite surfaces will be hydroxylated and have a hydration layer that extends from the solid into the solution. MgO dissolution is believed to occur by first converting to brucite [19,20]. A flocculent, gel-like adherent film was observed on MgO crystals that were exposed to water for several months at a time. Eventually, the solid crystals would disappear altogether as dissolution proceeded, leaving behind a cloudy mass of material roughly the same shape as the original crystal. The observed film is assumed to be composed of disordered and extended polynuclear Mg oxide and hydroxide moieties and water, much like a gel. This film was not observed on MgO crystals that were exposed to water for shorter periods, or even the crystals that were exposed for 70 h, but it was likely still forming and had not yet become visible. After dehydration, the hydroxylated surface layer is at least 50 Å thick on the MgO crystals exposed to water for 7 h, based on photoelectron escape depth data for the hydroxide/oxide ratios and a simple two-layer model [21]. The thickness of the hydroxylated layers on crystals exposed for longer periods is expected to be greater.

Pu(IV), as neutral $Pu(OH)_4$, will diffuse through the gel-like layer and may become incorporated in the active crystal surface. Any Pu(IV) colloids that form near the dissolving brucite surface are likely to remain near the outermost layers, not readily diffusing through the gel because of their larger size. Experiments conducted with colloidal brucite and citric acid showed a drop in citrate adsorption as citrate concentration exceeded the surface capacity. Colloidal Pu(IV), if it forms, would probably likewise remain in the outermost layers. XPS data does not support the idea of colloid formation and sorption. Pu 4f binding energy measurements decreased near the surface, whereas measurements of colloidal material show higher binding energies. On the other hand, reduction of surface species exposed to X-rays and ultra-high vacuum has been observed frequently and also shows the same time dependence that was observed. Pu hydroxides are much less soluble [22,23] than Mg hydroxides [24,25] so remain with the solid. Upon dehydration, the gel-like layer re-solidifies with the incorporated Pu. A conceptual model illustrating this process is shown in Fig. 6.

The research presented here strengthens the technical basis for our stewardship of actinide materials, particularly Pu oxide or materials contaminated with Pu. These investigations directly

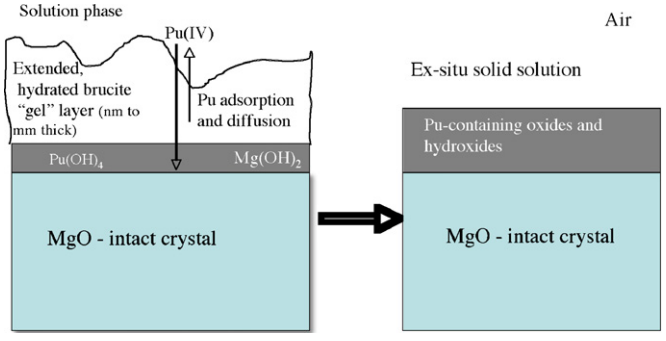

Fig. 6. Conceptual model of the Pu absorption process on MgO (1 0 0). Pu(IV) will diffuse through the gel-like layer and may become incorporated in the active crystal surface. Pu hydroxides are much less soluble than Mg hydroxides so remain with the solid. Upon dehydration the gel-like layer re-solidifies with the incorporated Pu.

support transuranic (TRU) waste disposal practices at the Waste Isolation Pilot Plant (WIPP). The DOE Performance Assessment states that Pu(IV) will be the dominant oxidation state under WIPP conditions in an intrusion scenario [26]. These experiments suggest that in a brine intrusion scenario, Pu(IV) will quickly become adsorbed and mineralized in the hydroxylated surface layers of the MgO backfill material. Pu may exist in higher oxidation states in localized regions where radiolysis produces sufficient quantities of oxidizing agents, but during any significant migration, the Pu(V) or Pu(VI) will likely be reduced under the influence of the prevailing basic and reducing solution conditions or as they are adsorbed on mineral surfaces [2]. Desorption of Pu is likely to be slower than adsorption on stable mineral surfaces [27], so as long as stable solids are present, Pu is likely to remain immobile. Colloids will be de-stabilized in the high ionic strength (8–9 M) of the WIPP. In effect, brucite will act like a Pu sponge. Pu ions adsorbed from water on brucite and hydroxylated MgO form compounds on and below the surface that share many of the same spectral features that have been observed on water-exposed Pu oxide, suggesting that Pu adsorbed on mineral surfaces will behave similarly.

Acknowledgements

Chris Wetteland and Yongquiang Wang of LANL provided RBS analysis. XANES and XAFS data are courtesy of Jeff Terry, formerly at LANL.

References

[1] D. Shaughnessy, et al., Environ. Sci. Technol. 37 (15) (2003) 3367–3374.
[2] A. Sanchez, J. Murray, T. Sibley, Geochim. Cosmochim. Acta 49 (11) (1985) 2297–2307.
[3] S. Kelly, et al., Environ. Sci. Technol. 37 (7) (2003) 1284–1287.
[4] N.C. Sturchio, et al., Science 281 (5379) (1998) 971–973.
[5] J. Davis, C. Fuller, A. Cook, Geochim. Cosmochim. Acta 51 (6) (1987) 1477–1490.
[6] S. Stipp, et al., Geochim. Cosmochim. Acta 56 (5) (1992) 1941–1954.
[7] B. Mincher, et al., Radiochim. Acta 91 (7) (2003) 397–401.
[8] M. Duff, et al., Environ. Sci. Technol. 33 (13) (1999) 2163–2169.
[9] J.D. Farr, R.K. Schulze, B.D. Honeyman, Radiochim. Acta 88 (9–11) (2000) 675–679.
[10] D.T. Larson, J. Vac. Sci. Technol. 17 (1) (1980) 55–58.
[11] J.D. Farr, R.K. Schulze, M.P. Neu, J. Nucl. Mater. 328 (2–3) (2004) 124–136.
[12] J.D. Farr, L.E. Cox, Los Alamos National Laboratory Report LA-11677-MS, 1989.
[13] V. Neck, J. Kim, Radiochim. Acta 89 (1) (2001) 1–16.
[14] T.W. Newton, V.L. Rundberg, Mater. Res. Soc. Symp. Proc. 26 (1984).
[15] J.F. Zeigler, J.P. Biersack, The Stopping and Range of Ions in Solids (TRIM), Pergamon Press, New York, 1985.
[16] S.D. Conradson, et al., Polyhedron 17 (4) (1998) 599–602.
[17] S. Conradson, et al., Inorg. Chem. 42 (12) (2003) 3715–3717.
[18] W. Runde, et al., Appl. Geochem. 17 (6) (2002) 837–853.
[19] R.A. Wogelius, et al., Geochim. Cosmochim. Acta 59 (9) (1995) 1875–1881.
[20] G. Jordan, S. Higgins, C. Eggleston, Am. Mineral. 84 (1–2) (1999) 144–151.
[21] M.P. Seah, W.A. Dench, Surf. Interface Anal. 1 (1) (1979) 2–11.
[22] H. Capdevila, P. Vitorge, Radiochim. Acta 82 (1998) 11–16.
[23] D. Rai, et al., Radiochim. Acta 89 (2) (2001) 67–74.
[24] D.A. Vermilyea, J. Electrochem. Soc. Electrochem. Sci. 116 (1969) 1179–1183.
[25] W. Stumm, J.J. Morgan, Aquatic Chemistry, second ed., John Wiley and Sons Inc., New York, 1981, pp. 270–273.
[26] USDOE96, Title 40 CFR Part 191 Compliance Certification Application for the Waste Isolation Pilot Plant, Appendix SOTERM, USDOE Carlsbad Area Office 1996-2184, 1996.
[27] N. Lu, et al., Radiochim. Acta 91 (12) (2003) 713–720.